

Radical concentrations, environments, and reactivities during crosslinking polymerizations

Kristi S. Anseth, Karin J. Anderson, Christopher N. Bowman*

Department of Chemical Engineering, University of Colorado, Boulder, Colorado 80309-0424, USA

(Received: April 3, 1995; revised manuscript of August 16, 1995)

SUMMARY:

Radical environments and concentrations during the crosslinking polymerizations of multiethylene glycol dimethacrylates were characterized with electron spin resonance spectroscopy. The relative concentrations of free and trapped radicals were used as a measure of certain structural features in the evolving polymer, especially with respect to microgel formation. The influence of monomer structure and crosslinking density on the polymer structure was studied by examining the radical behavior during the polymerization of diethylene glycol dimethacrylate, poly(ethylene glycol 200) dimethacrylate, and poly(ethylene glycol 600) dimethacrylate. The extent of radical trapping and microgel formation was found to increase with increasing crosslinking density. The influence of the rate of initiation on radical trapping was also investigated, and slower rates of polymerization led to a higher fraction of trapped radicals with respect to the total radical population. Finally, the termination mechanism of radicals was characterized (long-term and short-term) and the corresponding kinetic constants quantified.

Introduction

Photopolymerizations of multifunctional monomers provide a fast, solvent free technique to produce strong, dimensionally stable, crosslinked polymer coatings. Poly(diacrylates) and poly(dimethacrylates) have been extensively used in the coatings industry for optical fibers, microelectronic devices, and both aesthetic and abrasion resistant coatings^{1–3}. While the property requirements for the final coating vary widely and depend on the particular application, the long term performance and stability of the material are important issues. Such issues are strongly dependent on the polymer structure and changes that occur in the polymer structure with time.

Thus, it is highly desirable to characterize the structure of densely crosslinked polymers formed from the polymerization of multifunctional monomers; however, the complexity of the polymer structure has precluded the development of a complete network description. The primary reason for this difficulty is related to the heterogeneous nature of the polymerization process which forms the network. In particular, during the polymerization of multifunctional monomers, microgels of highly crosslinked polymers form within regions of a much lower crosslinking density^{4–6}. Microgels form as a result of the formation of highly crosslinked regions near the site of the initiated radicals.

Many experimental approaches have been used to characterize different aspects of the network structure and structural heterogeneity. Examples of these techniques include positron annihilation lifetime spectroscopy (PALS)^{7–9}, mobility sensitive

fluorescent¹⁰⁻¹⁵⁾ and photochromic probes¹⁶⁻²²⁾, and various scattering techniques^{23,24)}. In particular, the fluorescent and photochromic probing techniques have been most useful in characterizing the evolution of the polymer structure during polymerization. However, both techniques require the addition of probe molecules to the system which may affect the environment it is sensing.

In an alternative approach, this work attempts to characterize the evolution and structure of the polymer network by studying the concentration and mobility of radical species during the photopolymerization of multifunctional monomers. Specifically, electron spin resonance (ESR) spectroscopy was used to trace directly the concentration, behavior and environment of the radical species during photopolymerizations of multiethylene glycol dimethacrylates. Since ESR provides a direct measure of both the radical concentration and environment, radical species can be characterized as trapped or mobile, and the relative fractions in each state quantified. The fraction of trapped radicals and the variation in this fraction with polymerization time provides important information related to the formation of microgels and the degree of heterogeneity in the system.

In addition to monitoring radical concentrations and environments during the polymerization, post-polymerization studies of changes in the radical species provide details surrounding the influence of chemical aging (or post reaction) on the polymer structure. The presence of trapped radicals in crosslinked and/or glassy polymers has been widely observed^{1,25-32)}. In densely crosslinked poly(dimethacrylates), trapped radicals with lifetimes of several days or months have been observed, and these lifetimes were found to depend highly on the polymer crosslinking density²⁸⁻³¹⁾. Kloosterboer et al.²⁵⁾ photopolymerized 1,6-hexanediol diacrylate (HDDA) and bis(2-hydroxyethyl)bisphenol-A dimethacrylate (HEBDM) and found radical lifetimes exceeding 5 months at room temperature and under vacuum. These radicals remained trapped and stable even in the presence of large amounts of unreacted monomer and pendant double bonds.

Trapped radicals also present certain implications with respect to the long-term properties of the polymer. In particular, these radicals can react further with unreacted double bonds. This post-polymerization can lead to brittleness or stress development in the polymer. Alternatively, the radicals can react with diffusing oxygen molecules to form peroxides. Some work suggests that this peroxide forming reaction might account for the inferior long term mechanical properties of polymers produced from photopolymerizations as compared to thermal polymerizations.

This work determines the radical concentration profiles as a function of reaction time and conversion during the photopolymerization of a series of multiethylene glycol dimethacrylates. The radical species were also characterized as trapped or mobile depending on the local environment of the radical. This local radical environment was used as a measure of microgel formation and macrogelation in the polymer. In addition to studying radical concentrations and environments, termination kinetic constants and termination mechanisms of the radical species were determined. Finally, studies on the trapped radicals were performed to characterize the mechanism of their much slower termination rate.

Background

Atherton et al.³³⁾ and Bamfort et al.³⁴⁾ used ESR to provide some of the first experimental results of radical concentrations as a function of polymerization time. They also investigated the influence of crosslinking on radical trapping. Since these early studies, significant advancements in ESR techniques have led to further applications in studying and characterizing radical polymerizations. In particular, ESR sensitivity has improved to measure radical concentrations near 10^{-7} mol/L which are present at low conversions during radical polymerizations. Rapid scanning techniques have enabled the detection of fast changes in radical concentrations during dark and post-polymerizations. Polymerizations can be monitored *in situ*, so there is no need to quench the reaction with liquid nitrogen and subsequently measure the radical concentrations. Finally, spectra interpretation for polymerizing systems has significantly advanced through continually improving simulations and models.

Kamachi³⁵⁾ provides an excellent review of the applications of ESR spectroscopy to the radical polymerizations of vinyl compounds and presents studies on propagating radicals in both frozen and solid states. In terms of (meth)acrylate polymerizations, many researchers^{27, 35-37)} have studied the polymerization kinetics of methyl methacrylate with ESR. These studies were used to provide a direct measurement of the propagation and termination kinetic constants during this linear polymerization. Some of the most extensive work on crosslinking polymerizations of methacrylate networks has been done by Hamielec and coworkers copolymerizing methyl methacrylate (MMA) with ethylene glycol dimethacrylate (EGDMA).

As part of their work on the systematic study of crosslinking polymerizations, Hamielec and coworkers^{28, 31)} measured radical concentrations during thermal polymerizations of MMA/EGDMA copolymers of varying compositions. Radical concentrations of 10^{-7} to 10^{-3} mol/L were observed, and in general, as the amount of crosslinking monomer in the system was increased, the overall radical concentration increased. This radical concentration increase was due in part to the trapping of radicals which were chemically bound to the network. The radical concentration measurements were also coupled to conversion data to give a direct measurement of the propagation kinetic constant. Assuming that termination occurred exclusively by reaction diffusion at higher conversions, the initiation efficiency and termination kinetic constant were also determined. The initiation efficiency was found to behave closely to the propagation kinetic constant with a nearly constant efficiency at low conversion followed by a dramatic decrease at the same conversion where propagation became diffusion controlled.

In addition to studying radical concentrations and reactivities during polymerizations, Hamielec and coworkers^{29, 30)} have also investigated the trapping and termination of radicals in crosslinked polymers. As the crosslinking density in the polymer was increased, the final stable radical concentrations increased by nearly two orders of magnitude from 10^{-5} mol/L in pure poly(MMA) to 10^{-3} mol/L in pure poly(EGDMA). Post-polymerization measurements of the bimolecular termination of these radicals were made and studied at elevated temperatures. Two separate radical populations were identified as active radicals and inactive radicals. Temperature

increases provided a means for transforming inactive radical species to active ones, and the bimolecular termination kinetic constant was simultaneously monitored. The results showed a decrease in the termination kinetic constant for active radicals as the crosslinking density of the system was increased.

Finally, Hamielec and coworkers³¹⁾ have presented a model to simulate the ESR spectra of radicals during the copolymerization of methyl methacrylate and ethylene glycol dimethacrylate. Such models aid in clarifying the relationship between spectra and radical conformations, environments and reactivities. The simulation suggests that ESR spectra observed during the polymerization are a superposition of spectra arising from two types of radicals: a liquid-phase radical which give rise to a 13-line spectrum and a solid-phase radical with a slightly different 9-line spectrum. As polymerization proceeds from very low to high conversions, the ESR spectrum changes from a 13-line to a 9-line pattern. At intermediate conversions, the spectra is a superposition of both the 13-line and 9-line pattern which is the result of the heterogeneous nature of the crosslinking polymerization. Radicals coexist in monomer-rich regions and polymer microgel environments. These microgels can be glassy at relatively low conversions in systems with a high concentration of double bonds.

Tonge et al.³²⁾ provide an alternative interpretation for the 13-line and 9-line spectra of radical species in methacrylate polymerizations. Their studies indicate that the distinctions between the 13-line and 9-line spectra are based on the chain length and not the environment of the propagating radical. At low conversions, the 13-line spectrum arises from the superposition of the spectra of two similar rotamers. The rotamers are believed to be part of a very short kinetic chain or undergoing free rotation in a low viscosity medium. The 9-line spectrum was found to correspond to two rotamers of long-chain species of hindered, non-rotating polymer radicals.

Kloosterboer et al.²⁵⁾ have also examined the structure and stability of radicals trapped in polyacrylate networks. A significant fraction of these radicals was found to be stable even after thermal treatments to 80 °C and 120 °C. The presence of oxygen, however, caused a rapid decay in radical concentrations at room temperature. These studies eluded to the influence of high initial radical concentrations ($\sim 10^{-3}$ mol/L) produced from mild irradiation on the long-term properties of the polymer.

Similar results were reported by Best and Kasai examining poly(1,6-hexanediol diacrylate) and poly(1,6-hexanediol dimethacrylate)²⁶⁾. In addition to the above mentioned studies, several researchers have successfully used ESR spectroscopy in studying cure processes³⁸⁻⁴⁴⁾ and chain dynamics and relaxations⁴⁵⁻⁴⁷⁾.

The objective of this work is to study the concentrations, environments, and reactivities of radicals during photopolymerizations of multifunctional monomers. These polymerizations produce very highly crosslinked networks which can lead to extensive radical trapping. The stability and concentrations of these trapped radicals provide important structural information about the network and the related material properties. In particular, we are interested in studying the relative fraction of trapped and mobile radicals, and the important implications trapping has with respect to microgel formation. These properties are studied as a function of the initiation rate, the monomer size, the polymerization time, and the temporal stability.

Experimental part

The multifunctional monomers chosen for study were diethylene glycol dimethacrylate (DEGDMA; Polysciences Inc., Warrington, PA), poly(ethylene glycol 200) dimethacrylate (PEG200DMA; Polysciences Inc., Warrington, PA) and poly(ethylene glycol 600) dimethacrylate (PEG600DMA; Polysciences Inc., Warrington, PA). Samples were prepared by dissolving 0.1 wt.-% of the photoinitiator 2,2-dimethoxy-2-phenylacetophenone (DMPA; Ciba Geigy, Hawthorne, NY) in each monomer. Low initiator concentrations were used to minimize the exponential decay in light intensity through thicker samples in the ESR tubes. Before monitoring the polymerization, samples were deoxygenated by bubbling nitrogen through the solutions for approximately 10 min under a nitrogen atmosphere.

The samples were then transported to 4 mm, o. d., quartz ESR tubes and sealed under a nitrogen atmosphere. A Bruker ESP 300E ESR spectrometer (Billerica, MA) was used to monitor the radical concentrations during the photopolymerization process. The photopolymerizations were initiated on-line with a 365 nm UV light source (Cole-Parmer, Niles, IL) which gave an intensity of 0.2 mW/cm² at the ESR sample cavity. Polymerizations were conducted at 25 °C.

The absolute radical concentrations were calibrated with 2,2-diphenyl-1-picrylhydrazyl hydrate (DPPH; Aldrich, Milwaukee, WI). Standard solutions of DPPH in benzene were prepared with radical concentrations ranging from 10⁻⁷ mol/L to 10⁻³ mol/L. During polymerization, entire radical spectra were recorded frequently to monitor the details of the reaction; however, in some cases the changes in the radical concentrations were so rapid that the entire spectra could not be scanned. In these instances, the magnetic field was fixed at the frequency of the central line peak, and the changes in the peak height were related to the relative changes in the radical concentrations.

The polymerization profile and conversion were determined with differential scanning photocalorimetry. Monomer-photoinitiator solutions were placed in the cell of a differential scanning calorimeter (DSC) equipped with a photocalorimetric accessory (Perkin-Elmer, DSC-DPA 7, Norwalk, CT). The photocalorimetric accessory was equipped with a monochromator and neutral density filters, so the photopolymerization condition of 0.2 mW/cm² of 365 nm UV light in the ESR cavity could be replicated in the DSC cell. Before exposing the samples to the UV light, the DSC cell was flushed with nitrogen for 10 min. While not exact, the DSC experiments provided a reasonable mapping of the conversion profiles in the ESR cavity. Polymerization conditions were carefully replicated, and the time dependence for the rapid build-up of radical concentration as measured by the ESR corresponded well to the autoaccelerating rate measured with the DSC. The rate of polymerization was related to the heat flux monitored by the DSC, and the conversion was determined from the theoretical heat evolved per methacrylate double bond, $\Delta H_{\text{theor}} = 13.1 \text{ kcal/mol}^{48-50}$.

Results and discussion

Fig. 1 shows the typical ESR spectra that were collected while monitoring the homopolymerization of multiethylene glycol dimethacrylates. From the spectra several characteristic features of these radical polymerizations can be observed. In Fig. 1 a, taken 60 s into the polymerization, a characteristic 13-line spectrum is apparent, while in Fig. 1 b, taken after 500 s of polymerization, a 9-line spectrum of radicals in a glassy or solid environment is observed. At intermediate polymerization times, the spectra are undergoing transition from the 13-line to 9-line spectrum. In general, this transition was rather sharp in these densely crosslinked systems. The build-up of trapped radicals is rapid after the onset of gelation (at less than 2% conversion), which leads to a

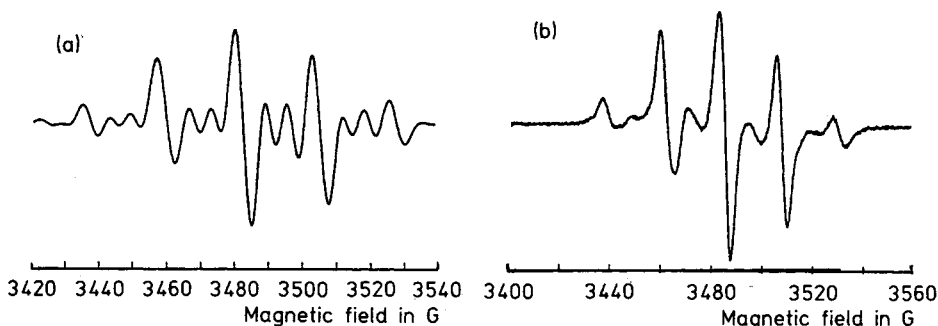


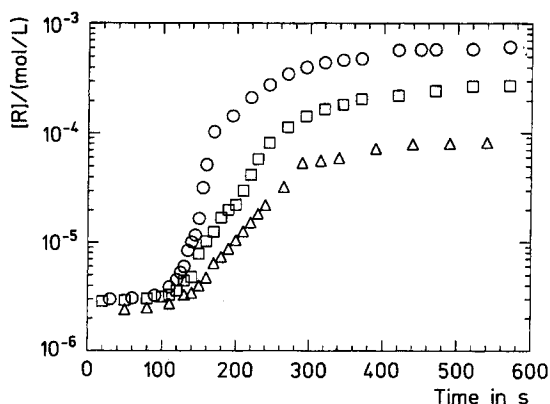
Fig. 1. Typical ESR spectra during the homopolymerization of multiethylene glycol dimethacrylates: (a) characteristic 13-line spectrum and (b) characteristic 9-line spectrum

dominant 9-line spectrum. The transition is the result of two separate populations of radicals that exist during the polymerization, radicals in a liquid-like environment and radicals in an environment which restricts their mobility. These drastically differing radical environments have important implications with respect to the polymerization behavior and termination kinetics in these highly crosslinked systems.

In Fig. 2, the total radical concentration is plotted as a function of polymerization time for DEGDMA, PEG200DMA, and PEG600DMA. These polymerizations were initiated with 0.1 wt.-% DMPA and 0.2 mW/cm² of UV light. From the general shapes of the curves, several features of the polymerization are apparent. At the beginning of the polymerization, the radical concentration reaches a steady state value around 2×10^{-6} mol/L, and $d[R]/dt$ is approximately 0. This region corresponds to low double bond conversion (i. e., less than 10% conversion) and high mobility in the system. The ESR spectra in this region have the very distinctive 13-lines which is characteristic of radicals with high mobility. As polymerization continues, a rapid increase in the radical concentration is observed which corresponds to the autoaccelerating region in the rate of polymerization as measured by DSC. In this region, a superposition of the 13-line and 9-line spectra was observed. This transition suggests a rapid change in the fraction of radicals that are mobile and a subsequent rise in the trapped radical fraction.

In addition to observing the general polymerization characteristics, the influence of crosslinking density on the radical concentrations and profiles can be determined by comparing the curve for DEGDMA to PEG200DMA to PEG600DMA. In these monomers, the average number of ethylene glycol units between the methacrylate double bonds is increasing from 2 to 4.5 to 13.5, respectively. In Fig. 2, the dramatic increase in radical concentration is observed first in DEGDMA followed by PEG200DMA and then PEG600DMA. The higher concentration of double bonds in DEGDMA leads to a faster rate of polymerization at lower conversions, and the higher crosslinking density of DEGDMA corresponds to a lower system mobility at lower conversions as compared to PEG600DMA. Both of these effects lead to an earlier manifestation of diffusion controlled termination and autoacceleration.

Fig. 2. The total radical concentration, $[R]$, as a function of polymerization time for DEGDMA (\circ), PEG200DMA (\square), and PEG600DMA (\triangle). Polymerizations were initiated with 0.1 wt.-% DMPA and 0.2 mW/cm^2 of UV light



The final radical concentrations also vary significantly from $6 \times 10^{-4} \text{ mol/L}$ in DEGDMA to $8 \times 10^{-5} \text{ mol/L}$ in PEG600DMA. These final radical concentrations are an indication of the high concentrations of trapped radicals that are present in each system. During the polymerization of DEGDMA, the high crosslinking density of the polymer (even in the microgels at low conversion) leads to extensive radical trapping at short polymerization times. As a result of this dramatic reduction in the system mobility, bimolecular termination is severely hindered and radicals terminate primarily through trapping. However, in PEG600DMA, the much lower crosslinking density and higher system mobility delays the onset of autoacceleration. A much higher fraction of radicals formed at the beginning of the polymerization terminate bimolecularly rather than becoming trapped. The result is a significant decrease in the final fraction of trapped radicals in the polymer network. As expected, PEG200DMA exhibited a behavior that was intermediate to DEGDMA and PEG600DMA.

To characterize further the fraction of trapped radicals and how this fraction varied during polymerization, a series of dark experiments was performed. In the dark experiments, the samples were exposed to initiating light for a given length of time. After this time, the light was turned off and changes in the radical concentration were monitored during the dark period (i.e. in the absence of further initiation). Fig. 3 shows representative results from 3 such experiments conducted at different double bond conversions during the curing of DEGDMA. These experiments provided information related to the kinetics of the termination mechanism and the extent of radical trapping. For example, by monitoring the decay in the radical concentration, the second order bimolecular termination kinetic constant of the mobile radicals can be determined. After the mobile radicals bimolecularly terminate, the final stable radical concentration represents the fraction of radicals that were trapped. From Fig. 3, the concentration and fraction of trapped radicals dramatically increase with conversion. At 15% conversion when initiation has been stopped, the radical concentration decays nearly 80% of its original value leaving approximately $1 \times 10^{-6} \text{ mol/L}$ of radicals trapped. In contrast, near 45% conversion of double bonds, only a mere 10% decrease in the radical concentration is seen in the "dark". Thus, 90% of

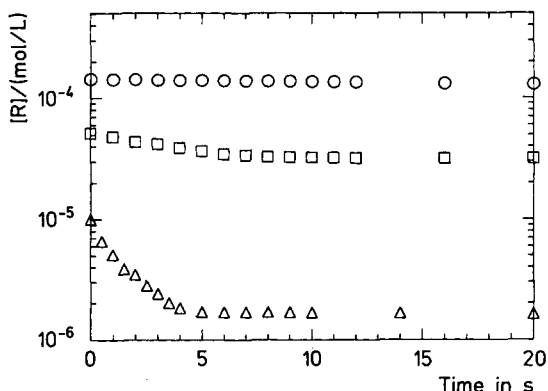


Fig. 3. The radical concentration, $[R]$, after initiation has ceased as a function of time where initiation was stopped at three different conversions: 45% (\circ), 30% (\square), and 15% (\triangle). Polymerizations were initiated with 0.1 wt.-% DMPA and 0.2 mW/cm^2 of UV light

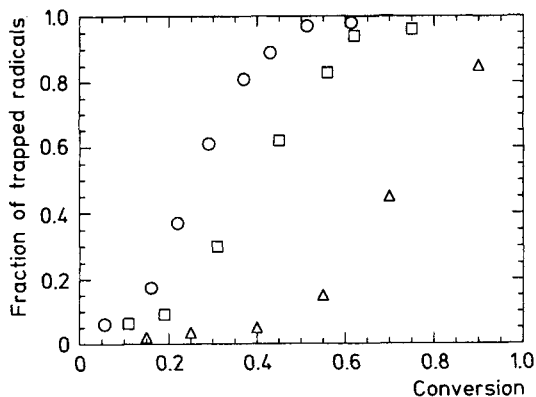


Fig. 4. The trapped radical fraction as a function of double bond conversion for DEGDMa (\circ), PEG200DMA (\square), and PEG600DMA (\triangle). The polymerizations were initiated with 0.1 wt.-% DMPA and 0.2 mW/cm^2 of UV light

the radicals are trapped (or immobile) in a polymerizing DEGDMa system at 45% conversion.

Fig. 4 plots the calculated trapped radical fraction as a function of double bond conversion for DEGDMa, PEG200DMA, and PEG600DMA. The polymerizations were initiated with 0.1 wt.-% DMPA and 0.2 mW/cm^2 of UV light, while the double bond conversions were determined from DSC experiments. The general shapes of the curves indicate three distinct regions. At low conversions, the majority of radicals are in liquid-like mobile environments, but a small fraction of trapped radicals is observable. The presence of trapped radicals at these low double bond conversions is evidence for the existence of highly crosslinked microgels in the system. From the data in this region, it would also appear that the extent of microgel formation is highest in DEGDMa and lowest in PEG600DMA as indicated by the relative fraction of trapped radicals in these systems.

The second region corresponds to the rapid rise in the trapped radical fraction. This sharp increase in the radical trapping is caused in part by the diffusion limitations on the polymeric radicals which lower the bimolecular termination kinetic constant and increase the probability of a radical becoming trapped. The increase in trapping is also indicative of the depletion of monomer pools as microgel regions grow together. At these higher conversions, the increased polymer fraction and, therefore, increased probability of entering a highly crosslinked polymer region, will greatly influence trapping. Previous kinetic studies^{51, 52)} in this region indicate that radical termination is occurring primarily by reaction diffusion. When reaction diffusion is the controlling termination mechanism, termination occurs by propagating through previously unreacted double bonds. Therefore, it is also likely that this propagation mechanism is becoming diffusion controlled in this region and leaving a greater fraction of radicals trapped and inactive for further polymerization. In comparing DEGDMA, PEG200DMA, and PEG600DMA, the trapped radical fraction increases first for DEGDMA (at $\approx 15\%$ double bond conversion) followed by PEG200DMA (at $\approx 25\%$) and PEG600DMA (at $\approx 60\%$). This delay in autoaccelerative radical trapping is indicative of the lower crosslinking density which imparts greater mobility to the system.

The last region of the curve is a plateau in the trapped radical fraction that is reached near the end of the polymerization. This plateau is observed around 50% conversion for DEGDMA, 60% conversion for PEG200DMA, and has not been reached in PEG600DMA at 90% conversion. This region is characterized by extremely limited mobility of all reacting species and the presence of a high fraction of trapped radicals. Only a limited fraction of radicals are mobile, and they are primarily the radicals that are initiated late in the polymerization. The observed increase in conversion results mainly from the new radicals that are initiated in the few remaining, small regions of monomer pools. The mobility and the relatively high concentration of double bonds in these regions allows the local radicals to further polymerize and increase conversion. Eventually, these monomer pools are consumed and the structure and mobility of the system limits further conversion. The limiting functional group conversion is 65% for DEGDMA, 80% for PEG200DMA, and 100% for PEG600DMA.

In addition, it is also informative to examine the trapped and free radical concentrations as a function of conversion. Fig. 5 shows the trapped and free radical concentrations, as a function of conversion for DEGDMA, PEG200DMA, and PEG600DMA. Polymerizations were initiated with 0.1 wt.-% DMPA and 0.2 mW/cm² of UV light. Initially, the trapped radical concentration is much lower than the free radical concentration. With continued polymerization, the trapped radical concentration increases monotonically while the free radical concentration approaches a maximum and then decreases. The behaviour seen in the free radical concentration is a result of changes in the system mobility which alter the radical termination mechanism.

At low conversions, the system mobility is high and initiation increases the concentration of free radicals in the system. The increase in the trapped radical concentration results mainly from the increase in the extent of polymer microgels in the system which shield the radicals from further polymerization. Unlike the concentration

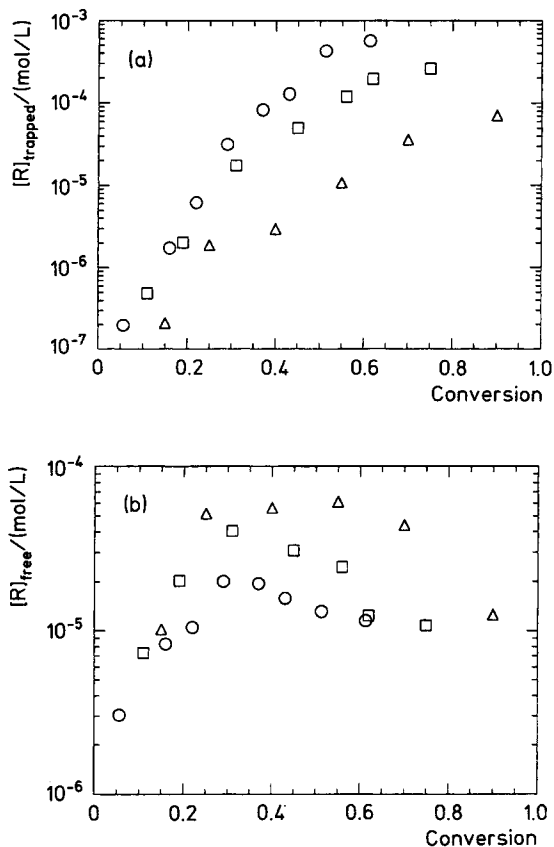
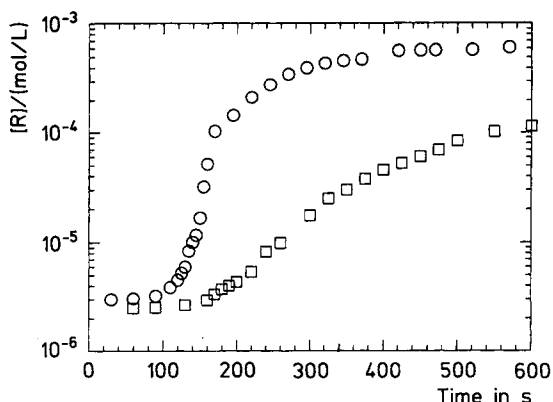


Fig. 5. The trapped (a) and free (b) radical concentrations ($[R]_{\text{trapped}}$ and $[R]_{\text{free}}$, resp.) as a function of conversion for the polymerization of DEGDMA (\circ), PEG200DMA (\square), and PEG600DMA (\triangle). Polymerizations were initiated with 0.1 wt.-% DMPA and 0.2 mW/cm² of UV light

of trapped radicals, the free radical concentration eventually reaches a maximum. At higher conversions, the mobility of the system is drastically reduced as the microgel regions now extend throughout the macroscopic gel. Initiation in areas of monomer pools continues to support the free radical population, but trapping of radicals is substantially increased because of the limited mobility in the system. The concentration of trapped radicals now begins to exceed the free radical concentration. With further diffusion limitations on species mobility, the free radical concentration begins to decrease. This decrease is the result of radical trapping. The behaviour exhibited in the trapped and free radical concentrations of DEGDMA, PEG200DMA, and PEG600DMA as a function of conversion supports the relationship between system mobility and the trapping of radicals in the polymerizing system.

In addition to studying the effects of monomer structure and crosslinking density on radical trapping, the influence of rate of polymerization was investigated. Fig. 6 presents the data for the total concentration of radicals as a function of polymerization time for DEGDMA polymerized at two different light intensities. Similar to the results shown in Fig. 2, the general shape of the curves indicates that a steady state radical

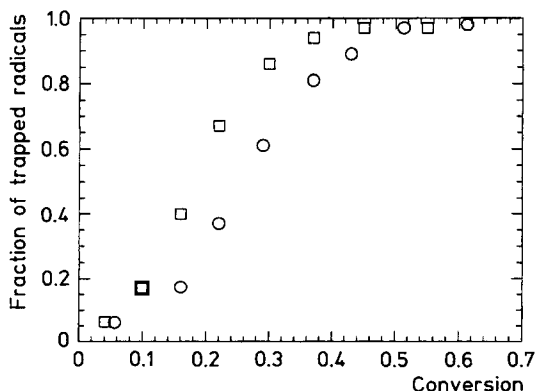
Fig. 6. The total concentration of radicals, $[R]$, as a function of polymerization time for DEGDMA polymerized at UV light intensities of 0.2 mW/cm^2 (\circ) and 0.02 mW/cm^2 (\square)



concentration is first reached. This is followed by autoacceleration and diffusion limited termination, and finally complete radical trapping and vanishing rates of polymerization. In addition to these general trends, the polymerization rate has an obvious effect on the radical concentrations. The system polymerized at the lower light intensity has correspondingly lower radical concentrations at all polymerization times, and the onset of autoacceleration is significantly delayed. Of further interest is the final radical concentration that is reached in each system which is $\approx 5 \times 10^{-4}$ at 0.2 mW/cm^2 and $\approx 1 \times 10^{-4}$ at 0.02 mW/cm^2 . This final radical concentration is important since it represents the final concentration of radicals that are trapped in the system. Thus, polymerizing at slower rates reduces the final concentration of trapped radicals.

In Fig. 7, the fraction of trapped radicals is plotted as a function of conversion for DEGDMA at two different light intensities. The trapped radical fractions were determined from similar dark experiments as described by Fig. 3. While slower initiation rates reduce the concentration of radicals that are trapped in the system, these results

Fig. 7. The fraction of trapped radicals as a function of conversion for DEGDMA polymerized at UV light intensities of 0.2 mW/cm^2 (\circ) and 0.02 mW/cm^2 (\square)



show that the fraction of radicals that are trapped is higher, especially in the auto-accelerative region. Thus, slower rates of initiation reduce the radical concentration to the point that the rate of termination by trapping increases relative to the rate of bimolecular termination. Whereas at faster rates of initiation, the higher radical concentration increases the rate of bimolecular termination, so the fraction of trapped radicals in these systems is actually lower. Eventually, both systems reach a conversion of reduced mobility and high polymer fraction where most of the radicals may be considered trapped. The effect of the rate of initiation on the trapped radical fraction has also been predicted with a kinetic gelation simulation and similar trends were reported⁵³).

The previous discussions have focused on characterizing the environment of the radicals, that is whether the radicals were mobile or trapped. In addition to this information, experiments were also conducted which monitored time dependent changes in the radical concentrations. In particular, valuable kinetic information was determined from the dark polymerization studies. During the dark polymerizations, initiation is absent, so the termination kinetic constant can be determined uniquely from the differential balance on the radical species. Assuming bimolecular termination is the dominating termination mechanism

$$\frac{d[R]}{dt} = -2k_{12}[R]^2 \quad (1)$$

where $[R]$ is the total radical concentration and k_{12} is the *average* bimolecular termination kinetic constant for all radical species. Thus, plots of $1/[R]$ versus time should provide information regarding this average bimolecular termination kinetic constant.

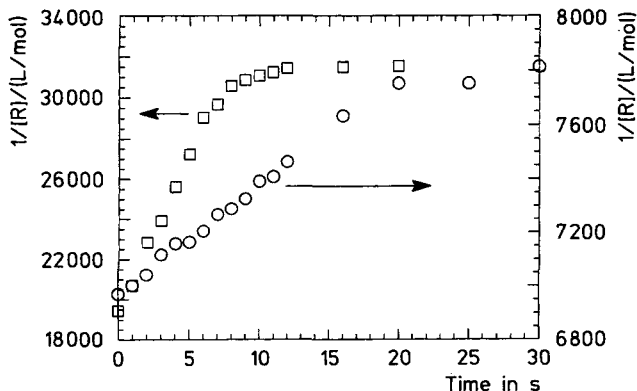


Fig. 8. The reciprocal radical concentration, $1/[R]$, as a function of time during the dark polymerization of DEGDMA where initiation was stopped at 30% (□) and 45% (○). The results are shown for the polymerization of DEGDMA at 0.2 mW/cm² and 0.1 wt.-% DMPA

In Fig. 8, the reciprocal radical concentration is plotted as a function of time for some of the dark polymerization experiments. From this figure, it appears that two different second order termination mechanisms are occurring. The first occurs on a relatively short time scale, whereas the second occurs over a much longer time period. The two time scales provide further evidence that two distinct radical termination mechanisms exist. Interestingly, both short and long term mechanisms are second order in the total radical concentration. This fact implies that all of the radicals terminate through the rapid mechanism and then undergo a transition and all of the radicals then terminate through a slower mechanism. The short term mechanism is assumed to be of the more mobile radicals and the termination kinetic constant for this reaction is referred to as $k_{t2, \text{mobile}}$.

From these results, the value of $k_{t2, \text{mobile}}$ at 30% conversion in DEGDMA was calculated as 720 L/(mol · s), while the value for $k_{t2, \text{mobile}}$ was 350 L/(mol · s) at 45% conversion. Other experimental techniques such as DSC and FTIR also provide a measurement of this termination kinetic constant of active radicals; however, ESR provides a measurement of the termination kinetic constants without assumptions related to the initiator efficiency or the pseudo steady-state approximation for the radical concentration. Of course, the reported termination kinetic constant is still an aggregate constant with a more complex dependence on the length of the polymer chains and the rate of reaction to that point.

An additional termination mechanism is the bimolecular termination of radicals which occurs on a much longer time scale than the polymerization. As previous figures have shown, extensive radical trapping occurs during the polymerization of multifunctional monomers. The radicals which terminate on the longer time scale are considered trapped with respect to the time scale of the polymerization. When examined over much longer periods of time (minutes rather than seconds), these “trapped” radicals terminate at a rate measurable by ESR. Characterization of this longer-term activity of trapped radicals is important as the system not only physically ages (i. e., volume relaxation), but also chemically ages (i. e., additional polymerization and termination), post-polymerization. For example, photo-cured coatings with a high concentration of trapped radicals after polymerization might become brittle because of post-curing in the sample.

Fig. 9 plots the changes in the trapped radical concentration normalized by the trapped radical concentration at the end of the polymerization as a function of time for poly(DEGDMA) and poly(PEG200DMA). Both polymerizations were initiated with 0.1 wt.-% DMPA and 0.25 mW/cm² of UV light. The systems were polymerized for 30 min and the maximum double bond conversion was reached in each system. For poly(DEGDMA), this maximum conversion was approximately 65% whereas for poly(PEG200DMA), the maximum was approximately 80%. The rate of termination of trapped radicals was highest in poly(DEGDMA) as observed by the larger fractional change in the trapped radical concentration. However, this faster rate of termination was attributed to the higher concentration of trapped radicals in poly(DEGDMA) as compared to poly(PEG200DMA) and not the magnitude of the termination kinetic constant. The trapped radical concentrations at the end of the polymerization of DEGDMA and PEG200DMA were 2.4×10^{-4} and 9.4×10^{-5} mol/L, respectively,

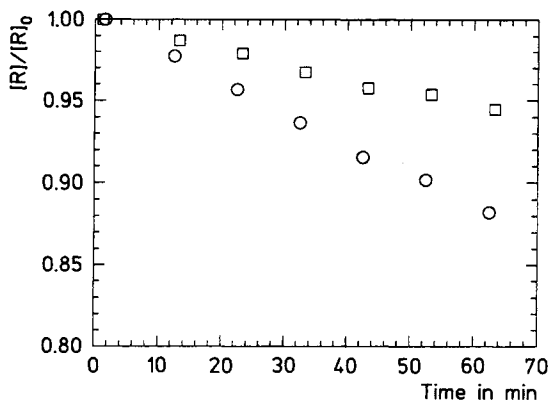


Fig. 9. The change in the trapped radical concentration normalized by the trapped radical concentration at the end of the polymerization as a function of time for poly(DEGDMA) (○) and poly(PEG200DMA) (□). The polymerizations were initiated with 0.1 wt.-% DMPA and 0.25 mW/cm² of UV light

whereas the termination kinetic constants were 10.1 L/(mol · s) (PEG200DMA) and 9.1 L/(mol · s) (DEGDMA). Hence, the termination kinetic constant was actually slightly lower in poly(DEGDMA) as might be expected since it is a more highly crosslinked system. The termination kinetic constants were determined by plotting the inverse radical concentration as a function of time, as in to Fig. 8.

The influence of polymerization rate on the long term kinetic constant was also studied by polymerizing DEGDMA and PEG200DMA at two different light intensities, 0.25 mW/cm² and 1.4 mW/cm². Tab. 1 summarizes the trapped radical concentrations at the end of the polymerization along with the termination kinetic constant for the radicals in these systems polymerized under different conditions. Clearly, faster rates of initiation (and thus polymerization) lead to a higher concentration of trapped radicals in the polymer network. Additionally, higher crosslinking densities of the network yield higher concentrations of trapped radicals in the polymer. In terms of the temporal stability of these radicals, the termination kinetic constants were quantified for each system. In general, the longer-term termination kinetic constants was one to two orders of magnitude smaller than the short term termination kinetic constant (which dominates on the time scale of the reaction).

Tab. 1. Summary of the trapped radical concentration immediately after polymerization, $[R]_0$, and the long-term termination kinetic constant, $k_{t, trap}$, and their dependence on the polymer network crosslinking density and maximum conversion

Polymer	Light intensity in mW/cm ²	Conversion	$[R]_0$ mol/L	$k_{t, trap}$ L/(mol · s)
poly(DEGDMA)	0.25	0.65	0.00024	9.1
	1.4	0.69	0.00040	2.9
poly(PEG200DMA)	0.25	0.79	0.000094	10.1
	1.4	0.80	0.00012	9.5

However, once polymerization is completed, the trapped radical concentrations can reach such high levels that the rate of trapped radical termination becomes significant and measurable. The longer-term termination kinetic constant depended on both the crosslinking density of the network and the rate of initiation, since faster rates of initiation lead to higher conversions in these systems. A more highly crosslinked network or a system at a higher conversion would have lower long-term termination kinetic constants for the trapped radicals.

Conclusions

Electron spin resonance spectroscopy was used to characterize the concentrations and mobilities of radicals during the crosslinking polymerizations of multiethylene glycol dimethacrylates. The MEGDMA monomers studied had average ethylene glycol bridge lengths ranging from 2 to 14.5. By studying this series of monomers, we were able to elucidate the effects of monomer structure and crosslinking density on the heterogeneity of the polymer. In particular, the extent of radical trapping was related to structural features of the network, such as microgel formation. The trapped radical fraction was investigated as a function of conversion, and systems of higher crosslinking density were found to have higher concentrations of trapped radicals. In addition, the effect of initiation rate on radical trapping was determined. The results showed that while faster rates of polymerization lead to higher trapped radical concentrations, slower rates of polymerization have a greater fraction of the total radical population that is trapped. Finally, the radical termination mechanism was studied on both short and long time scales. On the short time scale, this termination kinetic constant influences and controls the polymerization behavior and rate. In contrast, the longer time scale termination kinetic constant was indicative of the temporal stability of the trapped radicals which has important implications with respect to the aging and long-term performance of the polymeric material.

The authors wish to thank the National Science Foundation for the support of this work in the form of a grant (CTS-9209899), an REU to KJA, and a fellowship to KSA.

- 1) J. G. Kloosterboer, *Adv. Polym. Sci.* **84**, 1 (1988)
- 2) *Radiation Curing in Polymer Science and Technology, Volume IV: Practical Aspects and Applications*, J. P. Fouassier, J. F. Rabek, Eds., Elsevier, New York 1993
- 3) *Radiation Curing Science and Technology*, S. Peter Pappas, Ed., Plenum Press, New York 1992
- 4) A. Matsumoto, H. Ando, M. Oiwa, *Eur. Polym. J.* **25**, 185 (1989)
- 5) W. Funke, *Brit. Polym. J.* **21**, 107 (1989)
- 6) J. Bastide, L. Leibler, *Macromolecules* **21**, 2647 (1988)
- 7) J. Liu, Q. Deng, C. Jean, *Macromolecules* **26**, 7149 (1993)
- 8) Y. C. Jean, Q. Deng, *J. Polym. Sci., Part B* **30**, 1359 (1992)
- 9) K. Jeffrey, R. A. Pethrick, *Eur. Polym. J.* **30**, 153 (1994)
- 10) J. Paczkowski, D. C. Neckers, *Macromolecules* **25**, 548 (1992)

- 11) J. Paczkowski, D. C. Neckers, *J. Polym. Sci., Part A* **31**, 841 (1993)
- 12) T. Torii, H. Ushiki, K. Horie, *Polym. J.* **24**, 1057 (1992)
- 13) T. Torii, H. Ushiki, K. Horie, *Polym. J.* **25**, 173 (1993)
- 14) Y. Higuchi, S. Suyama, *Polym. J.* **24**, 1181 (1992)
- 15) M. Berghmans, S. Govaers, H. Berghmans, F. C. DeSchryver, *Polym. Eng. Sci.* **32**, 1466 (1992)
- 16) J. S. Royal, J. G. Victor, J. M. Torkelson, *Macromolecules* **25**, 729 (1992)
- 17) J. S. Royal, J. M. Torkelson, *Macromolecules* **25**, 4792 (1992)
- 18) K. S. Anseth, M. D. Rothenberg, C. N. Bowman, *Macromolecules* **27**, 2890 (1994)
- 19) W.-C. Yu, C. S. P. Sung, *Macromolecules* **21**, 365 (1988)
- 20) C. S. P. Sung, I. R. Gould, N. J. Turro, *Macromolecules* **17**, 1447 (1984)
- 21) K. Horie, K. Hirao, N. Kenmochi, I. Mita, *Makromol. Chem.* **9**, 267 (1988)
- 22) I. Mita, K. Horie, K. Hirao, *Macromolecules* **22**, 558 (1989)
- 23) R.-J. Roe, J. J. Curro, *Macromolecules* **16**, 428 (1983)
- 24) H. H. Song, R.-J. Roe, *Macromolecules* **20**, 2723 (1987)
- 25) J. G. Kloosterboer, G. F. C. M. Lijten, F. J. A. M. Greidanus, *Polym. Rep.* **27**, 269 (1986)
- 26) M. E. Best, P. H. Kasai, *Macromolecules* **22**, 2622 (1989)
- 27) R. W. Garrett, D. J. T. Hill, J. H. O'Donnell, P. J. Pomery, C. L. Winzor, *Polym. Bull (Berlin)* **22**, 611 (1989)
- 28) S. Zhu, Y. Tian, A. E. Hamielec, D. R. Eaton, *Polymer* **31**, 154 (1990)
- 29) S. Zhu, Y. Tian, A. E. Hamielec, D. R. Eaton, *Polymer* **31**, 1726 (1990)
- 30) S. Zhu, Y. Tian, A. E. Hamielec, D. R. Eaton, *Macromolecules* **23**, 1144 (1990)
- 31) Y. Tian, S. Zhu, A. E. Hamielec, D. B. Fulton, D. R. Eaton, *Polymer* **33**, 384 (1992)
- 32) M. P. Tonge, R. J. Pace, R. G. Gilbert, *Macromol. Chem. Phys.* **195**, 3159 (1994)
- 33) N. M. Atherton, H. W. Melville, D. H. Whiffen, *J. Polym. Sci.* **34**, 199 (1959)
- 34) C. H. Bamford, A. D. Jenkins, M. C. R. Symons, M. G. Townsend, *J. Polym. Sci.* **34**, 181 (1959)
- 35) M. Kamachi, *Adv. Polym. Sci.* **82**, 207 (1987)
- 36) S. E. Bresler, E. N. Kazbekov, V. N. Shadrin, *Makromol. Chem.* **175**, 2875 (1974)
- 37) M. J. Ballard, R. G. Gilbert, D. H. Napper, P. J. Pomery, J. H. O'Donnell, *Macromolecules* **17**, 504 (1984)
- 38) F. R. Tollens, L. J. Lee, *Polymer* **34**, 29 (1993)
- 39) E. S. Nefed'ev, V. A. Silaev, T. Yu. Mirakova, M. K. Kadirov, A. V. Il'yasov, *Polymer* **33**, 3911 (1992)
- 40) T. Sato, K. Masaki, M. Seno, H. Tanaka, *Makromol. Chem.* **194**, 849 (1993)
- 41) A. Kajiwara, Y. Konishi, Y. Morishima, W. Schmabel, K. Kuwata, M. Kamachi, *Macromolecules* **26**, 1656 (1993)
- 42) R. P. N. Veregin, M. K. Georges, P. M. Kazmaier, G. K. Hamer, *Macromolecules* **26**, 5316 (1993)
- 43) G. R. Cutting, B. J. Tabner, *Macromolecules* **26**, 951 (1993)
- 44) A. Matsumoto, K. Mizuta, *Macromolecules* **27**, 5863 (1994)
- 45) H. Yoshida, T. Ichikawa, *Adv. Polym. Sci.* **105**, 1 (1993)
- 46) J. Pilar, J. Labsky, *Macromolecules* **27**, 3977 (1994)
- 47) J. Rychly, L. Rychla, M. Klimova, *Polymer* **34**, 4961 (1993)
- 48) K. Miyazaki, T. J. Horibe, *J. Biomed. Mater. Res.* **22**, 1011 (1988)
- 49) K. Horie, A. Otagawa, M. Muraoka, I. Mita, *J. Polym. Sci.* **13**, 445 (1975)
- 50) J. E. Moore, in: *Chemistry and Properties of Crosslinked Polymers*, S. Labana, Ed., Academic Press, New York 1977, p. 535
- 51) K. S. Anseth, C. M. Wang, C. N. Bowman, *Macromolecules* **27**, 650 (1994)
- 52) K. S. Anseth, C. M. Wang, C. N. Bowman, *Polymer* **35**, 3243 (1994)
- 53) K. S. Anseth, C. N. Bowman, *J. Polym. Sci., Part B* **33**, 769 (1995)